

# THE QUANTIZED HALL EFFECT

Nobel lecture, December 9, 1985

by

KLAUS von KLITZING,

Max-Planck-Institut für Festkörperforschung, D-7000 Stuttgart 80

## 1. Introduction

Semiconductor research and the Nobel Prize in physics seem to be contradictory since one may come to the conclusion that such a complicated system like a semiconductor is not useful for very fundamental discoveries. Indeed, most of the experimental data in solid state physics are analyzed on the basis of simplified theories, and very often the properties of a semiconductor device is described by empirical formulas since the microscopic details are too complicated. Up to 1980 nobody expected that there exists an effect like the Quantized Hall Effect, which depends exclusively on fundamental constants and is not affected by irregularities in the semiconductor like impurities or interface effects.

The discovery of the Quantized Hall Effect (QHE) was the result of systematic measurements on silicon field effect transistors-the most important device in microelectronics. Such devices are not only important for applications but also for basic research. The pioneering work by Fowler, Fang, Howard and Stiles [1] has shown that new quantum phenomena become visible if the electrons of a conductor are confined within a typical length of 10 nm. Their discoveries opened the field of two-dimensional electron systems which since 1975 is the subject of a conference series [2]. It has been demonstrated that this field is important for the description of nearly all optical and electrical properties of microelectronic devices. A two-dimensional electron gas is absolutely necessary for the observation of the Quantized Hall Effect, and the realization and properties of such a system will be discussed in section 2. In addition to the quantum phenomena connected with the confinement of electrons within a two-dimensional layer, another quantization - the Landau quantization of the electron motion in a strong magnetic field - is essential for the interpretation of the Quantized Hall Effect (section 3). Some experimental results will be summarized in section 4 and the application of the QHE in metrology is the subject of section 5.

## 2 Two-Dimensional Electron Gas

The fundamental properties of the QHE are a consequence of the fact that the energy spectrum of the electronic system used for the experiments is a *discrete* energy spectrum. Normally, the energy  $E$  of mobile electrons in a

semiconductor is quasicontinuous and can be compared with the kinetic energy of free electrons with wave vector  $k$  but with an effective mass  $m^*$

$$E = \frac{\hbar^2}{2m^*} (k_x^2 + k_y^2 + k_z^2) \tag{1}$$

If the energy for the motion in one direction (usually  $z$ -direction) is fixed, one obtains a quasi-two-dimensional electron gas (2DEG), and a strong magnetic field perpendicular to the two-dimensional plane will lead-as discussed later-to a fully quantized energy spectrum which is necessary for the observation of the QHE.

A two-dimensional electron gas can be realized at the surface of a semiconductor like silicon or gallium arsenide where the surface is usually in contact with a material which acts as an insulator ( $\text{SiO}_2$  for silicon field effect transistors and, e.g.  $\text{Al}_x\text{Ga}_{1-x}\text{As}$  for heterostructures). Typical cross sections of such devices are shown in Fig 1. Electrons are confined close to the surface of the semiconductor by an electrostatic field  $F_z$  normal to the interface, originating from positive charges (see Fig. 1) which causes a drop in the electron potential towards the surface.

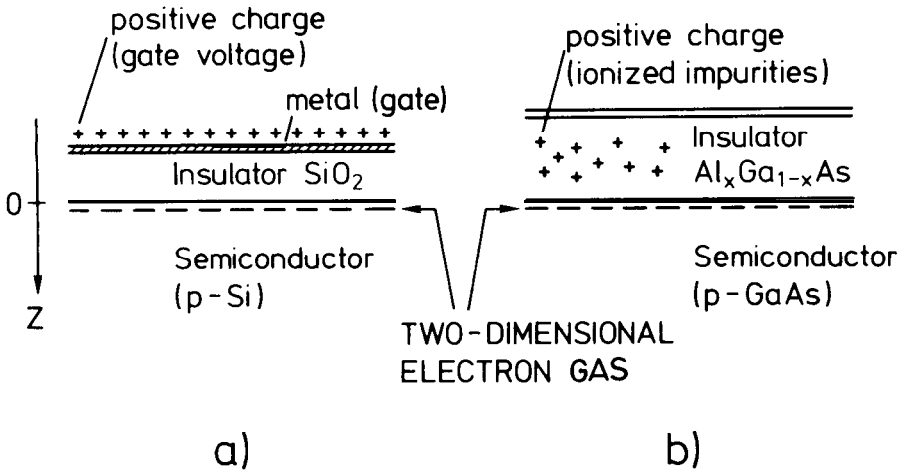


Fig. 1. A two-dimensional electron gas (2DEG) can be formed at the semiconductor surface if the electrons are fixed close to the surface by an external electric field. Silicon MOSFETs (a) and GaAs- $\text{Al}_x\text{Ga}_{1-x}\text{As}$  heterostructures (b) are typical structures used for the realization of a 2DEG.

If the width of this potential well is small compared to the de Broglie wavelength of the electrons, the energy of the carriers are grouped in so-called electric subbands  $E_i$  corresponding to quantized levels for the motion in  $z$ -direction, the direction normal to the surface. In lowest approximation, the electronic subbands can be estimated by calculating the energy eigenvalues of an electron in a triangular potential with an infinite barrier at the surface ( $z=0$ ) and a constant electric field  $F_z$  for  $z \geq 0$ , which keeps the electrons close to the surface. The result of such calculations can be approximated by the equation

$$E_j = \left( \frac{\hbar^2}{2m^*} \right)^{1/3} \cdot \left( \frac{3}{2} \pi e F_s \right)^{2/3} \cdot \left( j + \frac{3}{4} \right)^{2/3} \tag{2}$$

$j = 0, 1, 2 \dots$

In some materials, like silicon, different effective masses  $m^*$  and  $m^{*1}$  may be present which leads to different series  $E_j$  and  $E_j'$ .

Equation (2) must be incorrect if the energy levels  $E_j$  are occupied with electrons, since the electric field  $F_s$  will be screened by the electronic charge.

For a more quantitative calculation of the energies of the electric subbands it is necessary to solve the Schrödinger equation for the actual potential  $V_z$  which changes with the distribution of the electrons in the inversion layer. Typical results of such calculation for both silicon MOSFETs and GaAs-heterostructures are shown in Fig. 2 [3,4]. Usually, the electron concentration of the two-dimensional system is fixed for a heterostructure (Fig. 1 b) but can be varied in a MOSFET by changing the gate voltage.

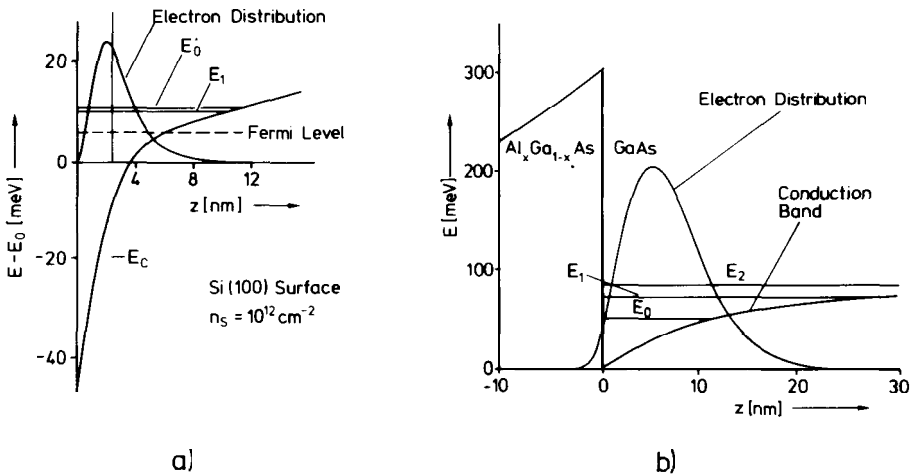


Fig. 2. Calculations of the electric subbands and the electron distribution within the surface channel of a silicon MOSFET (a) and a GaAs-Al<sub>x</sub>Ga<sub>1-x</sub>As heterostructure [3, 4].

Experimentally, the separation between electric subbands, which is of the order of 10 meV, can be measured by analyzing the resonance absorption of electromagnetic waves with a polarization of the electric field perpendicular to the interface [5].

At low temperatures ( $T < 4$  K) and small carrier densities for the 2DEG (Fermi energy  $E_f$  relative to the lowest electric subbands  $E_0$ , small compared with the subband separation  $E_1 - E_0$ ) only the lowest electric subband is occupied with electrons (electric quantum limit), which leads to a strictly two-dimensional electron gas with an energy spectrum

$$E = E_0 + \frac{\hbar^2 k_{||}^2}{2m^*} \tag{3}$$

where  $k_{||}$  is a wavevector within the two-dimensional plane.

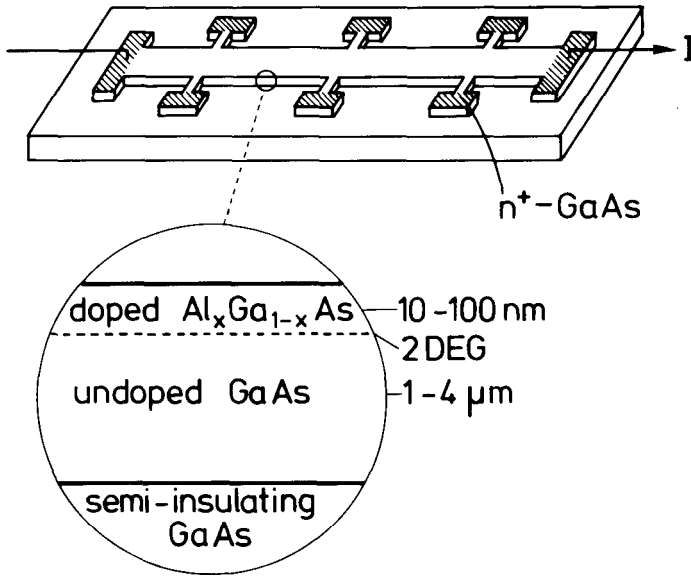


Fig. 3. Typical shape and cross-section of a GaAs-Al<sub>x</sub>Ga<sub>1-x</sub>As heterostructure used for Hall effect measurements.

For electrical measurements on a 2DEG, heavily doped n<sup>+</sup>-contacts at the semiconductor surface are used as current contacts and potential probes. The shape of a typical sample used for QHE-experiments (GaAs-heterostructure) is shown in Fig. 3. The electrical current is flowing through the surface channel, since the fully depleted Al<sub>x</sub>Ga<sub>1-x</sub>As acts as an insulator (the same is true for the SiO<sub>2</sub> of a MOSFET) and the p-type semiconductor is electrically separated from the 2DEG by a p-n junction. It should be noted that the sample shown in Fig. 3 is basically identical with new devices which may be important for the next computer generation [6]. Measurements related to the Quantized Hall Effect which include an analysis and characterization of the 2DEG are therefore important for the development of devices, too.

### 3. Quantum Transport of a 2DEG in Strong Magnetic Fields

A strong magnetic field  $B$  with a component  $B_z$ , normal to the interface causes the electrons in the two-dimensional layer to move in cyclotron orbits parallel to the surface. As a consequence of the orbital quantization the energy levels of the 2DEG can be written schematically in the form

$$E_n = E_0 + (n + 1/2)\hbar\omega_c + s \cdot g \cdot \mu_B \cdot B$$

$$n = 0, 1, 2, \dots$$
(4)

with the cyclotron energy  $\hbar\omega_c = \hbar eB/m^*$ , the spin quantum numbers  $s = \pm 1/2$  the Landé factor  $g$  and the Bohr magneton  $\mu_B$ .

The wave function of a 2DEG in a strong magnetic field may be written in a form where the y-coordinate  $y_0$  of the center of the cyclotron orbit is a good quantum number [7].

$$\psi = e^{ikx} \Phi_n(y - y_0)$$
(5)

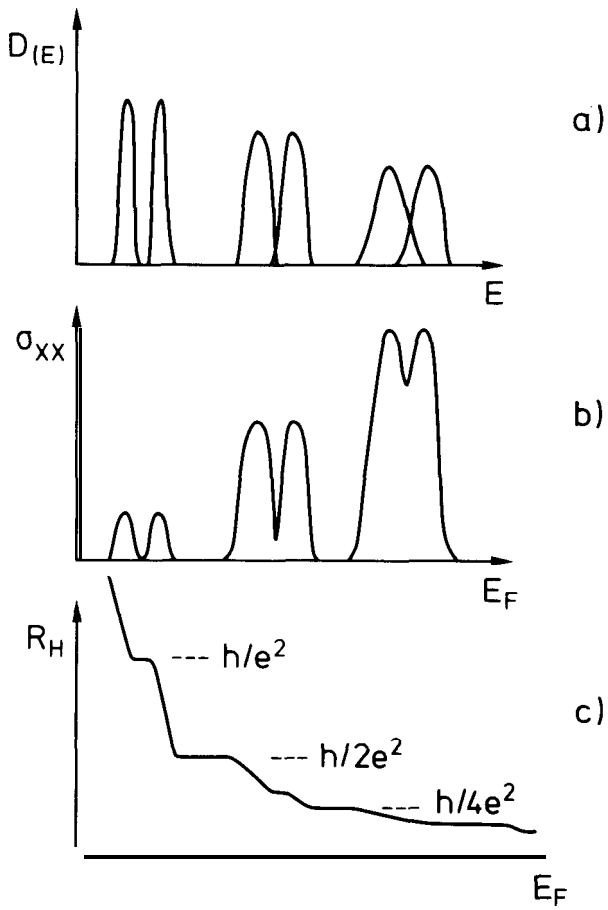


Fig. 4. Sketch for the energy dependence of the density of states (a), conductivity  $\sigma_{xx}$  (b), and Hall resistance  $R_H$  (c) at a fixed magnetic field.

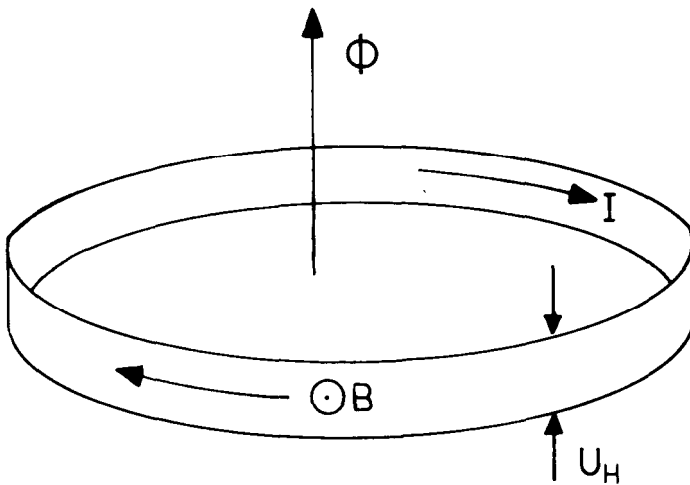


Fig. 5. Model of a two-dimensional metallic loop used for the derivation of the quantized Hall resistance.

where  $\Phi_n$  is the solution of the harmonic-oscillator equation

$$\frac{1}{2m^*} [p_y^2 + (eB)^2 y^2] \Phi_n = (n + \frac{1}{2}) \hbar \omega_c \Phi_n \quad (6)$$

and  $y_0$  is related to  $k$  by

$$y_0 = \hbar k / eB \quad (7)$$

The degeneracy factor for each Landau level is given by the number of center coordinates  $y_0$  within the sample. For a given device with the dimension  $L_x$ ,  $L_y$ , the center coordinates  $y_0$  are separated by the amount

$$\Delta y_0 = \frac{\hbar}{eB} \Delta k = \frac{\hbar}{eB} \frac{2\pi}{L_x} = \frac{h}{eBL_x} \quad (8)$$

so that the degeneracy factor  $N_0 = L_y / \Delta y_0$  is identical with  $N_0 = L_x L_y eB / h$  the number of flux quanta within the sample. The degeneracy factor per unit area is therefore:

$$N = \frac{N_0}{L_x L_y} = \frac{eB}{h} \quad (9)$$

It should be noted that this degeneracy factor for each Landau level is independent of semiconductor parameters like effective mass.

In a more general way one can show [8] that the commutator for the center coordinates of the cyclotron orbit  $[x_0, y_0] = i\hbar / eB$  is finite, which is equivalent to the result that each state occupies in real space the area  $F_0 = h / eB$  corresponding to the area of a flux quantum.

The classical expression for the Hall voltage  $U_H$  of a 2DEG with a surface carrier density  $n_s$  is

$$U_H = \frac{B}{n_s \cdot e} \cdot I \quad (10)$$

where  $I$  is the current through the sample. A calculation of the Hall resistance  $R_H = U_H / I$  under the condition that  $i$  energy levels are fully occupied ( $n_s = iN$ ), leads to the expression for the quantized Hall resistance

$$R_H = \frac{B}{iN \cdot e} = \frac{h}{ie^2} \quad (11)$$

$$i = 1, 2, 3$$

*A quantized Hall resistance is always expected if the carrier density  $n_s$  and the magnetic field  $B$  are adjusted in such a way that the filling factor  $i$  of the energy Levels (Eq. 4)*

$$i = \frac{n_s}{eB/h} \quad (12)$$

*is an integer.*

Under this condition the conductivity  $\sigma_{xx}$  (current flow in the direction of the electric field) becomes zero since the electrons are moving like free particles exclusively perpendicular to the electric field and no diffusion (originating from

scattering) in the direction of the electric field is possible. Within the self-consistent Born approximation [9] the discrete energy spectrum broadens as shown in Fig. 4a. **This theory predicts that the conductivity  $\sigma_{xx}$  is mainly proportional to the square of the density of states at the Fermi energy  $E$ , which leads to a vanishing conductivity  $\sigma_{xx}$  in the quantum Hall regime and quantized plateaus in the Hall resistance  $R_H$  (Fig. 4c).**

**The simple one-electron picture for the Hall effect of an ideal two-dimensional system in a strong magnetic field leads already to the correct value for the quantized Hall resistance (Eq. 11) at integer filling factors of the Landau levels. However, a microscopic interpretation of the QHE has to include the influences of the finite size of the sample, the finite temperature, the electron-electron interaction, impurities and the finite current density (including the inhomogeneous current distribution within the sample) on the experimental result. Up to now, no corrections to the value  $h/e^2$  of the quantized Hall resistance are predicted if the conductivity  $\sigma_{xx}$  is zero. Experimentally,  $\sigma_{xx}$  is never exactly zero in the quantum Hall regime (see section 4) but becomes unmeasurably small at high magnetic fields and low temperatures. A quantitative theory of the QHE has to include an analysis of the longitudinal conductivity  $\sigma_{xx}$  under real experimental conditions, and a large number of publications are discussing the dependence of the conductivity on the temperature, magnetic field, current density, sample size etc. The fact that the value of the quantized Hall resistance seems to be exactly correct for  $\sigma_{xx} = 0$  has led to the conclusion that the knowledge of microscopic details of the device is not necessary for a calculation of the quantized value. Consequently Laughlin [10] tried to deduce the result in a more general way from gauge invariances. He considered the situation shown in Fig. 5. A ribbon of a two-dimensional system is bent into a loop and pierced everywhere by a magnetic field  $B$  normal to its surface. A voltage drop  $U_H$  is applied between the two edges of the ring. Under the condition of vanishing conductivity  $\sigma_{xx}$  (no energy dissipation), energy is conserved and one can write Faraday's law of induction in a form which relates the current  $I$  in the loop to the adiabatic derivative of the total energy of the system  $E$  with respect to the magnetic flux  $\Phi$  threading the loop**

$$I = \frac{\partial E}{\partial \Phi} \quad (13)$$

If the flux is varied by a flux quantum  $\Phi_0 = h/e$ , the wavefunction enclosing the flux must change by a phase factor  $2\pi$  corresponding to a transition of a state with wavevector  $k$  into its neighbour state  $k + (2\pi) / (L_x)$ , where  $L_x$  is the circumference of the ring. The total change in energy corresponds to a transport of states from one edge to the other with

$$\Delta E = i \cdot e \cdot U_H \quad (14)$$

The integer  $i$  corresponds to the number of filled Landau levels if the free electron model is used, but can be in principle any positive or negative integer number.

From Eq. (13) the relation between the dissipationless Hall current and the Hall voltage can be deduced

$$I = i \cdot e \cdot U_H / \Phi_0 = i \frac{e}{\hbar} \cdot U_H \quad (15)$$

which leads to the quantized Hall resistance  $R_H = \frac{\hbar}{ie^2}$ .

In this picture the main reason for the Hall quantization is the flux quantization  $h/e$  and the quantization of charge into elementary charges  $e$ . In analogy, the fractional quantum Hall effect, which will not be discussed in this paper, is interpreted on the basis of elementary excitations of quasiparticles with a charge  $e^* = \frac{e}{3}, \frac{e}{5}, \frac{e}{7}$  etc.

The simple theory predicts that the ratio between the carrier density and the magnetic field has to be adjusted with very high precision in order to get exactly integer filling factors (Eq. 12) and therefore quantized values for the Hall resistance. Fortunately, the Hall quantization is observed not only at special magnetic field values but in a wide magnetic field range, so that an accurate fixing of the magnetic field or the carrier density for high precision measurements of the quantized resistance value is not necessary. Experimental data of such Hall plateaus are shown in the next section and it is believed that localized states are responsible for the observed stabilization of the Hall resistance at certain quantized values.

After the discovery of the QHE a large number of theoretical papers were published discussing the influence of localized states on the Hall effect [11 - 14] and these calculations demonstrate that the Hall plateaus can be explained if localized states in the tails of the Landau levels are assumed. Theoretical investigations have shown that a mobility edge exists in the tails of Landau levels separating extended states from localized states [15-18]. The mobility edges are located close to the center of a Landau level for long-range potential fluctuations. Contrary to the conclusion reached by Abrahams, et al [19] that all states of a two-dimensional system are localized, one has to assume that in a strong magnetic field at least one state of each Landau level is extended in order to observe a quantized Hall resistance. Some calculations indicate that the extended states are connected with edge states [17].

In principle, an explanation of the Hall plateaus without including localized states in the tails of the Landau levels is possible if a reservoir of states is present outside the two-dimensional system [20, 21]. Such a reservoir for electrons, which should be in equilibrium with the 2DEG, fixes the Fermi energy within the energy gap between the Landau levels if the magnetic field or the number of electrons is changed. However, this mechanism seems to be more unlikely than localization in the tails of the Landau levels due to disorder. The following discussion assumes therefore a model with extended and localized states within one Landau level and a density of states as sketched in Fig. 6.



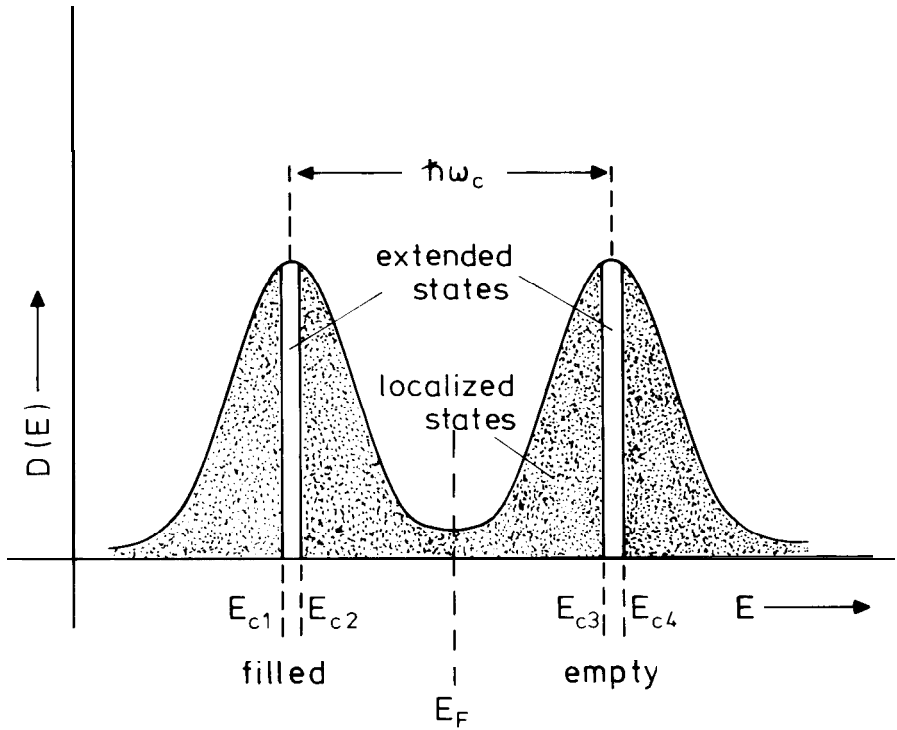


Fig. 6. Model for the broadened density of states of a 2 DEG in a strong magnetic field. Mobility edges close to the center of the Landau levels separate extended states from localized states.

#### 4. Experimental Data

Magnetoquantum transport measurements on two-dimensional systems are known and published for more than 20 years. The first data were obtained with silicon MOSFETs and at the beginning mainly results for the conductivity  $\sigma_{xx}$  as a function of the carrier density (gate voltage) were analyzed. A typical curve is shown in Fig. 7. The conductivity oscillates as a function of the filling of the Landau levels and becomes zero at certain gate voltages  $V_g$ . In strong magnetic fields  $\sigma_{xx}$  vanishes not only at a fixed value  $V_g$  but in a range  $\Delta V_g$ , and Kawaji was the first one who pointed out that some kind of immobile electrons must be introduced [22], since the conductivity  $\sigma_{xx}$  remains zero even if the carrier density is changed. However, no reliable theory was available for a discussion of localized electrons, whereas the peak value of  $\sigma_{xx}$  was well explained by calculations based on the self-consistent Born approximation and short-range scatterers which predict  $\sigma_{xx} \sim (n + 1/2)$  independent of the magnetic field.

The theory for the Hall conductivity is much more complicated, and in the lowest approximation one expects that the Hall conductivity  $\sigma_{xy}$  deviates from the classical curve  $\sigma_{xy}^0 = -\frac{n_s e}{B}$  (where  $n_s$  is the total number of electrons in the two-dimensional system per unit area) by an amount  $\Delta\sigma_{xy}$  which depends mainly on the third power of the density of states at the Fermi energy [23].

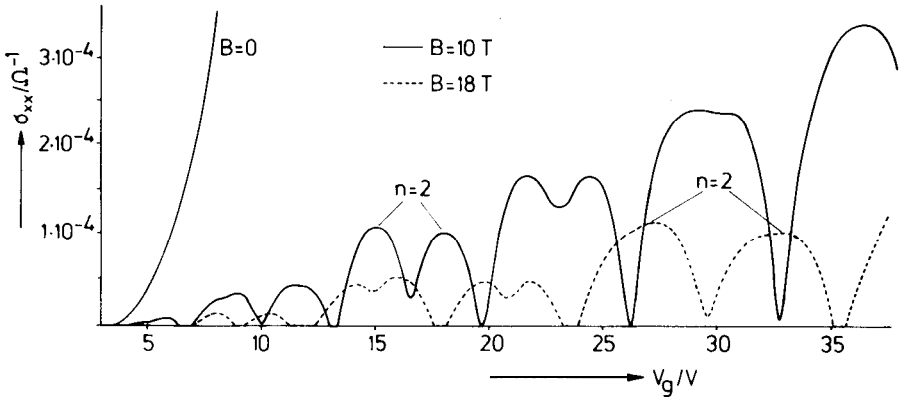


Fig. 7. Conductivity  $\sigma_{xx}$  of a silicon MOSFET at different magnetic fields  $B$  as a function of the gate voltage  $V_g$ .

However, no agreement between theory and experiment was obtained. Today, it is believed, that  $\Delta\sigma_{xy}$  is mainly influenced by localized states, which can explain the fact that not only a positive but also a negative sign for  $\Delta\sigma_{xy}$  is observed. Up to 1980 all experimental Hall effect data were analyzed on the basis of an incorrect model so that the quantized Hall resistance, which is already visible in the data published in 1978 [24] remained unexplained.

Whereas the conductivity  $\sigma_{xx}$  can be measured directly by using a Corbino disk geometry for the sample, the Hall conductivity is not directly accessible in an experiment but can be calculated from the longitudinal resistivity  $\rho_{xx}$  and the Hall resistivity  $\rho_{xy}$  measured on samples with Hall geometry (see Fig. 3):

$$\sigma_{xy} = \frac{\rho_{xy}}{\rho_{xx}^2 + \rho_{xy}^2}, \quad \sigma_{xx} = \frac{\rho_{xx}}{\rho_{xx}^2 + \rho_{xy}^2} \tag{16}$$

Fig. 8 shows measurements for  $\rho_{xx}$  and  $\rho_{xy}$  of a silicon MOSFET as a function of the gate voltage at a fixed magnetic field. The corresponding  $\sigma_{xx}$ - and  $\sigma_{xy}$ -data are calculated on the basis of Eq. (16).

The classical curve  $\sigma_{xy}^0 = -\frac{n_s c}{B}$  in Fig. 8 is drawn on the basis of the incorrect model, that the experimental data should lie always below the classical curve (= fixed sign for  $\Delta\sigma_{xy}$ ) so that the plateau value  $\sigma_{xy} = \text{const.}$  (observable in the gate voltage region where  $\sigma_{xx}$  becomes zero) should change with the width of the plateau. Wider plateaus should give smaller values for  $|\sigma_{xy}|$ . The main discovery in 1980 was [23] that the value of the Hall resistance in the plateau region is not influenced by the plateau width as shown in Fig. 9. Even the aspect ratio  $L/W$  ( $L$  = length,  $W$  = width of the sample), which influences normally the accuracy in Hall effect measurements, becomes unimportant as shown in Fig. 10. Usually, the measured Hall resistance  $R_H^{\text{exp}}$  is always smaller than the theoretical value  $R_H^{\text{theor}} = \rho_{xy}$  [ 26, 27]

$$R_H^{\text{exp}} = G \cdot R_H^{\text{theor}} \quad G < 1 \tag{17}$$

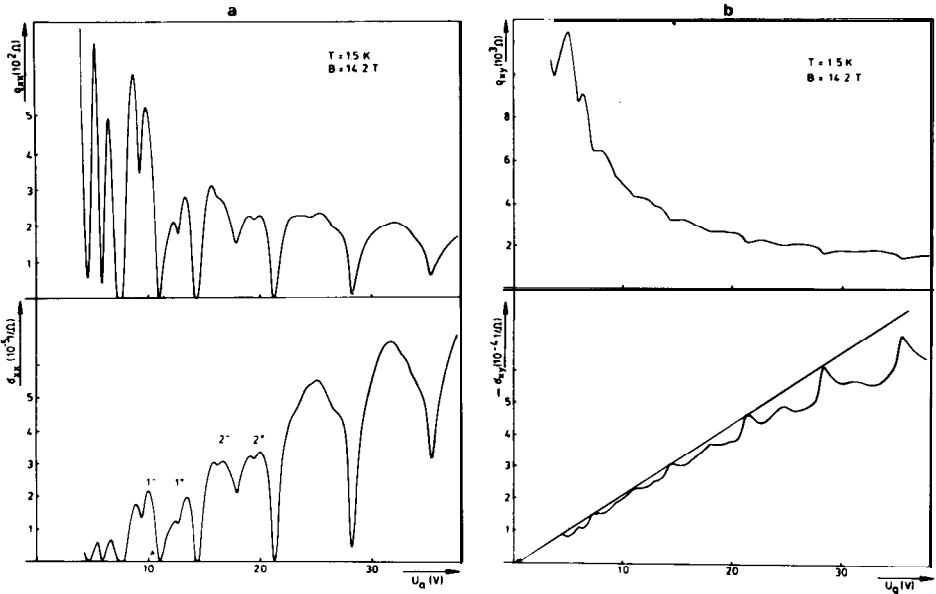


Fig. 8. Measured  $Q_{xx}$ - and  $Q_{xy}$ -data of a silicon MOSFET as a function of the gate voltage at  $B = 14.2$  together with the calculated  $\sigma_{xx}$ - and  $\sigma_{xy}$ -curves.

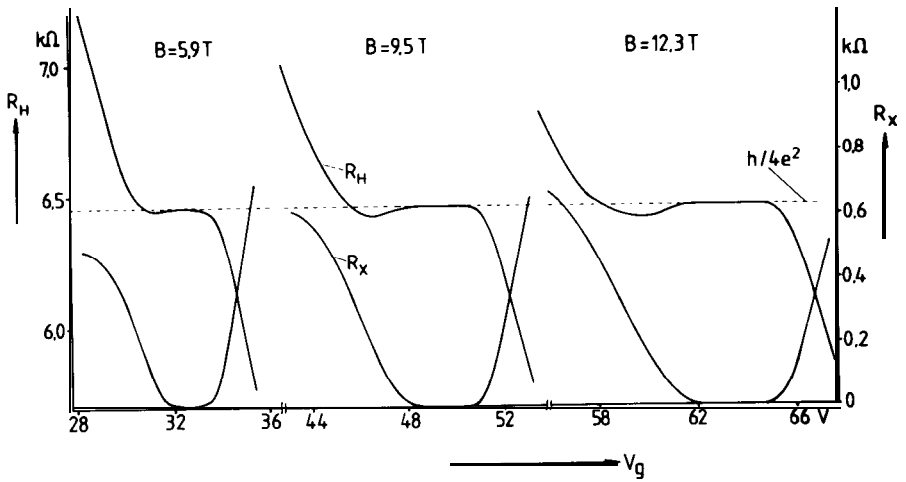


Fig. 9. Measurements of the Hall resistance  $R_H$  and the resistivity  $R_x$  as a function of the gate voltage at different magnetic field values. The plateau values  $R_H = h/4e^2$  are independent of the width of the plateaus.

However, as shown in Fig. 11, the correction  $1-G$  becomes zero (independent of the aspect ratio) if  $\sigma_{xx} \rightarrow 0$  or the Hall angle  $\theta$  approaches  $90^\circ$  ( $\tan \theta = \frac{v_{xy}}{v_{xx}}$ ).

This means that any shape of the sample can be used in QHE-experiments as long as the Hall angle is  $90^\circ$  (or  $\sigma_{xx} = 0$ ). However, outside the plateau region

( $\sigma_{xx} \sim \rho_{xx} \neq 0$ ) the measured Hall resistance  $R_H^{exp} = \frac{U_H}{I}$  is indeed always

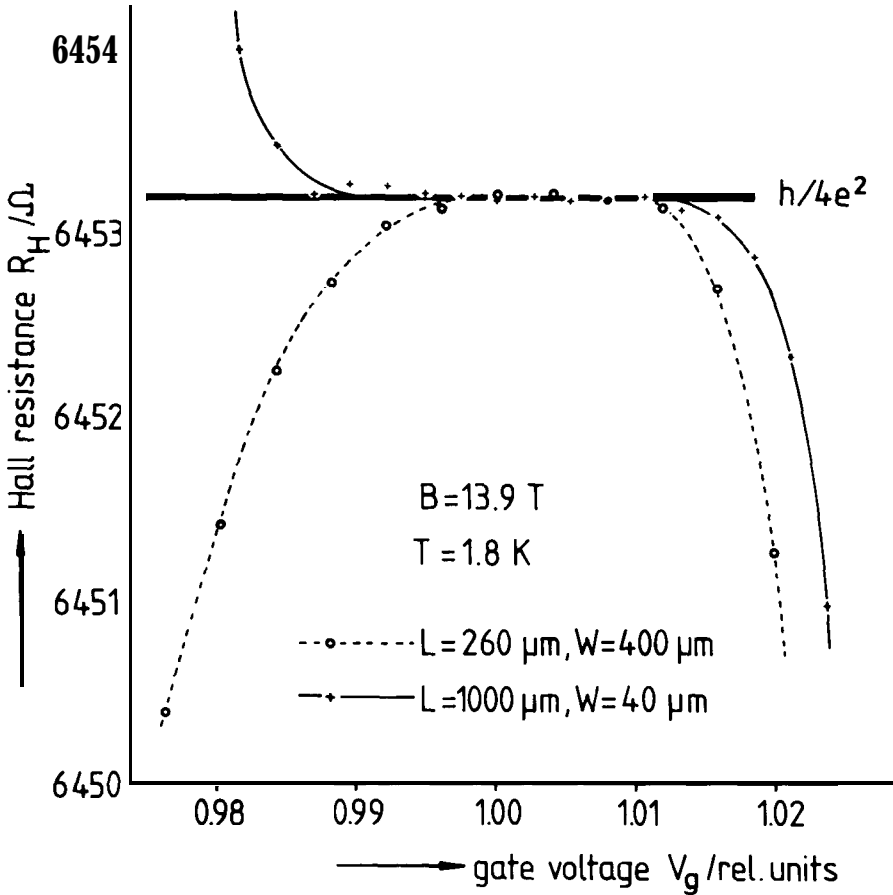


Fig. 10. Hall resistance  $R_H$  for two different samples with different aspect ratios  $L/W$  as a function of the gate voltage ( $B = 13.9 \text{ T}$ ).

smaller than the theoretical  $\rho_{xy}$  value [28]. This leads to the experimental result that an additional minimum in  $R_H^{\text{exp}}$  becomes visible outside the plateau region as shown in Fig. 9, which disappears if the correction due to the finite length of the sample is included (See Fig. 12). The first high-precision measurements in 1980 of the plateau value in  $R_H(V_g)$  showed already that these resistance values are quantized in integer parts of  $h/e^2 = 25812.8 \Omega$  within the experimental uncertainty of 3 ppm.

The Hall plateaus are much more pronounced in measurements on GaAs- $\text{Al}_x\text{Ga}_{1-x}\text{As}$  heterostructures, since the small effective mass  $m^*$  of the electrons in GaAs ( $m^*(\text{Si})/m^*(\text{GaAs}) > 3$ ) leads to a relatively large energy splitting between Landau levels (Eq. 4), and the high quality of the GaAs- $\text{Al}_x\text{Ga}_{1-x}\text{As}$  interface (nearly no surface roughness) leads to a high mobility  $\mu$  of the electrons, so that the condition  $\mu B > 1$  for Landau quantizations is fulfilled already at relatively low magnetic fields. Fig. 13 shows that well-developed Hall plateaus are visible for this material already at a magnetic field strength of 4 tesla. Since a finite carrier density is usually present in heterostructures, even

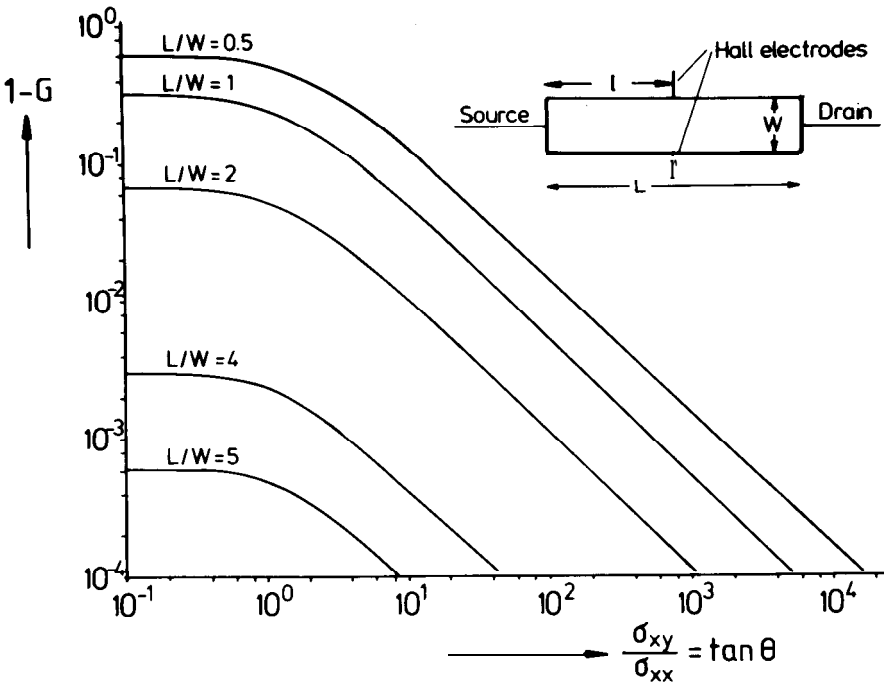


Fig. 11. Calculations of the correction term  $G$  in Hall resistance measurements due to the finite length to width ratio  $L/W$  of the device ( $l/L = 0.5$ ).

at a gate voltage  $V_g = 0V$ , most of the published transport data are based on measurements without applied gate voltage as a function of the magnetic field. A typical result is shown in Fig. 14. The Hall resistance  $R_H = \rho_{xy}$  increases steplike with plateaus in the magnetic field region where the longitudinal resistance  $\rho_{xx}$  vanishes. The width of the  $\rho_{xx}$ -peaks in the limit of zero temperature can be used for a determination of the amount of extended states and the analysis [29] shows, that only few percent of the states of a Landau level are not localized. The fraction of extended states within one Landau level decreases with increasing magnetic field (Fig. 15) but the number of extended states within each level remains approximately constant since the degeneracy of each Landau level increases proportionally to the magnetic field.

At finite temperatures  $\rho_{xx}$  is never exactly zero and the same is true for the slope of the  $\rho_{xy}$ -curve in the plateau region. But in reality, the slope  $d\rho_{xy}/dB$  at  $T < 2K$  and magnetic fields above 8 Tesla is so small that the  $\rho_{xy}$ -value stays constant within the experimental uncertainty of  $6 \cdot 10^{-8}$  even if the magnetic field is changed by 5 %. Simultaneously the resistivity  $\rho_{xx}$  is usually smaller than  $1m\Omega$ . However, at higher temperatures or lower magnetic fields a finite resistivity  $\rho_{xx}$  and a finite slope  $d\rho_{xy}/dn_s$  (or  $d\rho_{xy}/dB$ ) can be measured. The data are well described within the model of extended states at the energy position of the undisturbed Landau level  $E_n$  and a finite density of localized states between the Landau levels (mobility gap). Like in amorphous systems, the temperature dependence of the conductivity  $\sigma_{xx}$  (or resistivity  $\rho_{xx}$ ) is thermally activated

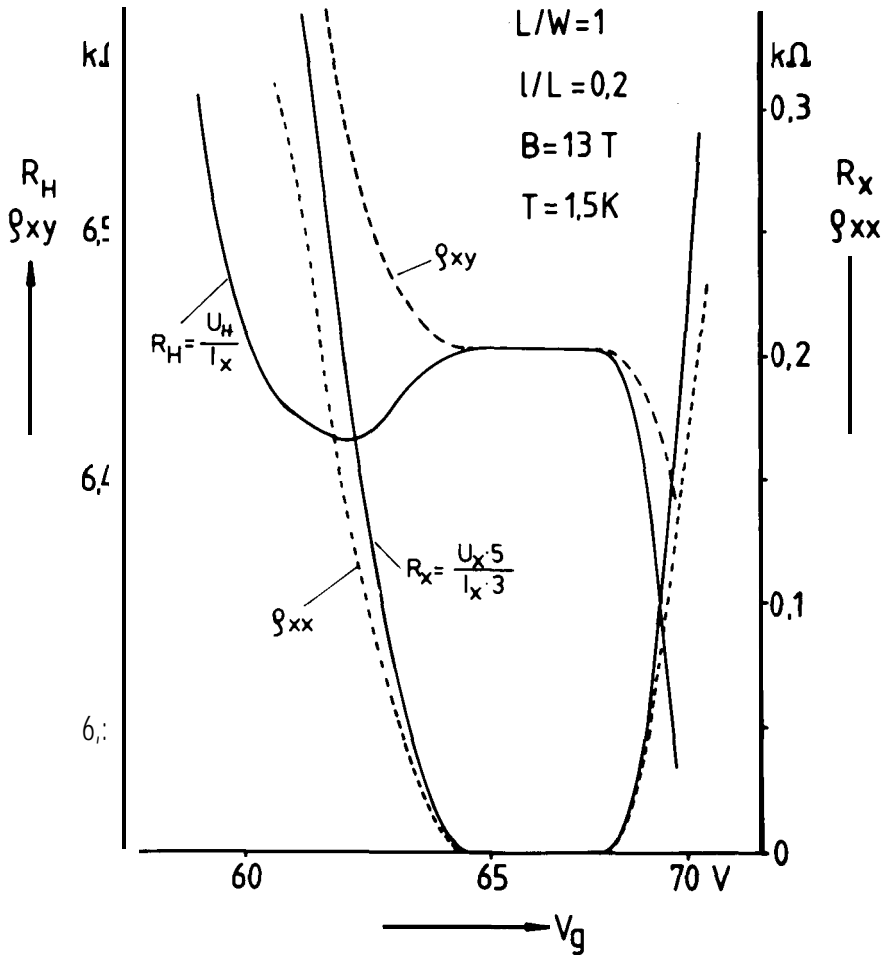


Fig. 12. Comparison between the measured quantities  $R_H$  and  $R_x$  and the corresponding resistivity components  $Q_{xy}$  and  $Q_{xx}$ , respectively.

with an activation energy  $E_a$  corresponding to the energy difference between the Fermi energy  $E_F$  and the mobility edge. The largest activation energy with a value  $E_a = 1/2 \hbar \omega_c$  (if the spin splitting is negligibly small and the mobility edge is located at the center  $E_n$  of a Landau level) is expected if the Fermi energy is located exactly at the midpoint between two Landau levels.

Experimentally, an activated resistivity

$$Q_{xx} \sim \exp[-(E_a/kT)] \tag{18}$$

is observed in a wide temperature range for different two-dimensional systems (deviations from this behaviour, which appear mainly at temperatures below 1K, will be discussed separately) and a result is shown in Fig. 16. The activation energies (deduced from these data) are plotted in Fig. 17 for both, silicon MOSFETs and GaAs-Al<sub>x</sub>Ga<sub>1-x</sub>As heterostructures as a function of the

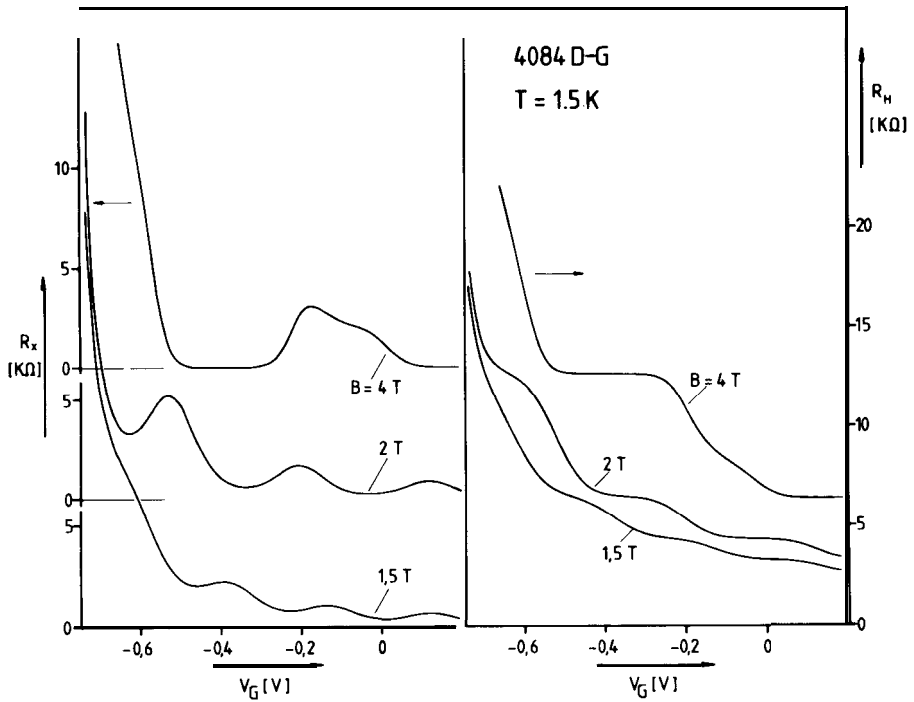


**Fig. 13.** Measured curves for the Hall resistance  $R_H$  and the longitudinal resistance  $R_x$  of a GaAs-AlGaAs heterostructure as a function of the gate voltage at different magnetic fields.

magnetic field and the data agree fairly well with the expected curve  $E_n = 1/2\hbar\omega_c$ . Up to now, it is not clear whether the small systematic shift of the measured activation energies to higher values originates from a temperature dependent prefactor in Eq. (18) or is a result of the enhancement of the energy gap due to many body effects.

The assumption, that the mobility edge is located close to the center of a Landau level  $E_n$  is supported by the fact that for the samples used in the experiments only few percent of the states of a Landau level are extended [29]. From a systematic analysis of the activation energy as a function of the filling factor of a Landau level it is possible to determine the density of states  $D(E)$  [30]. The surprising result is, that the density of states (DOS) is finite and approximately constant within 60% of the mobility gap as shown in Fig. (18). This background DOS depends on the electron mobility as summarized in Fig. (19).

An accurate determination of the DOS close to the center of the Landau level is not possible by this method since the Fermi energy becomes temperature dependent if the DOS changes drastically within the energy range of  $3kT$ . However, from an analysis of the capacitance  $C$  as a function of the Fermi energy the peak value of the DOS and its shape close to  $E_n$  can be deduced [31, 32].

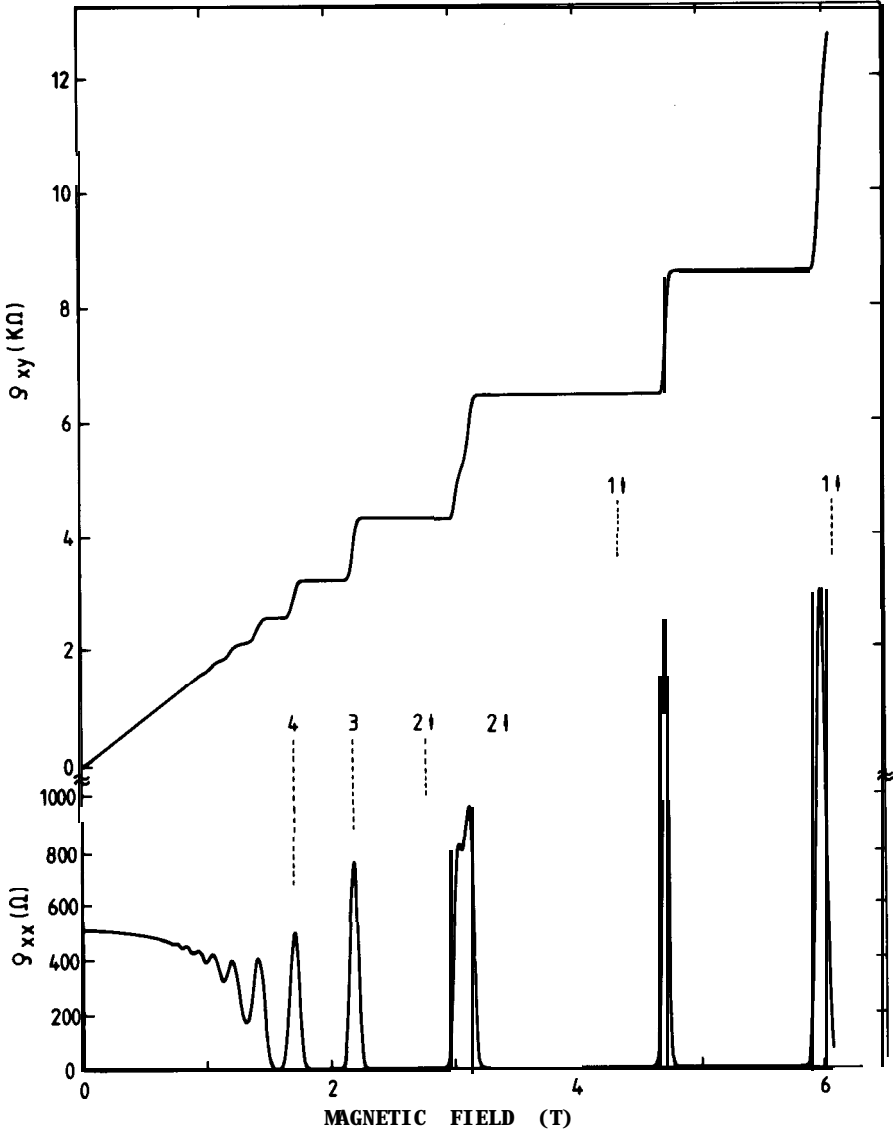


Fig. 14. Experimental curves for the Hall resistance  $R_H = Q_{xy}$  and the resistivity  $Q_{xx} \sim R_x$  of a heterostructure as a function of the magnetic field at a fixed carrier density corresponding to a gate voltage  $V_g = 0V$ . The temperature is about 8mK.

This analysis is based on the equation

$$\frac{1}{C} = \frac{1}{e^2 \cdot D(E_F)} + \text{const.} \tag{19}$$

The combination of the different methods for the determination of the DOS leads to a result as shown in Fig. (20). Similar results are obtained from other experiments, too [33, 34] but no theoretical explanation is available.

If one assumes that only the occupation of extended states influences the Hall effect, than the slope  $dQ_{xy}/dn_s$  in the plateau region should be dominated



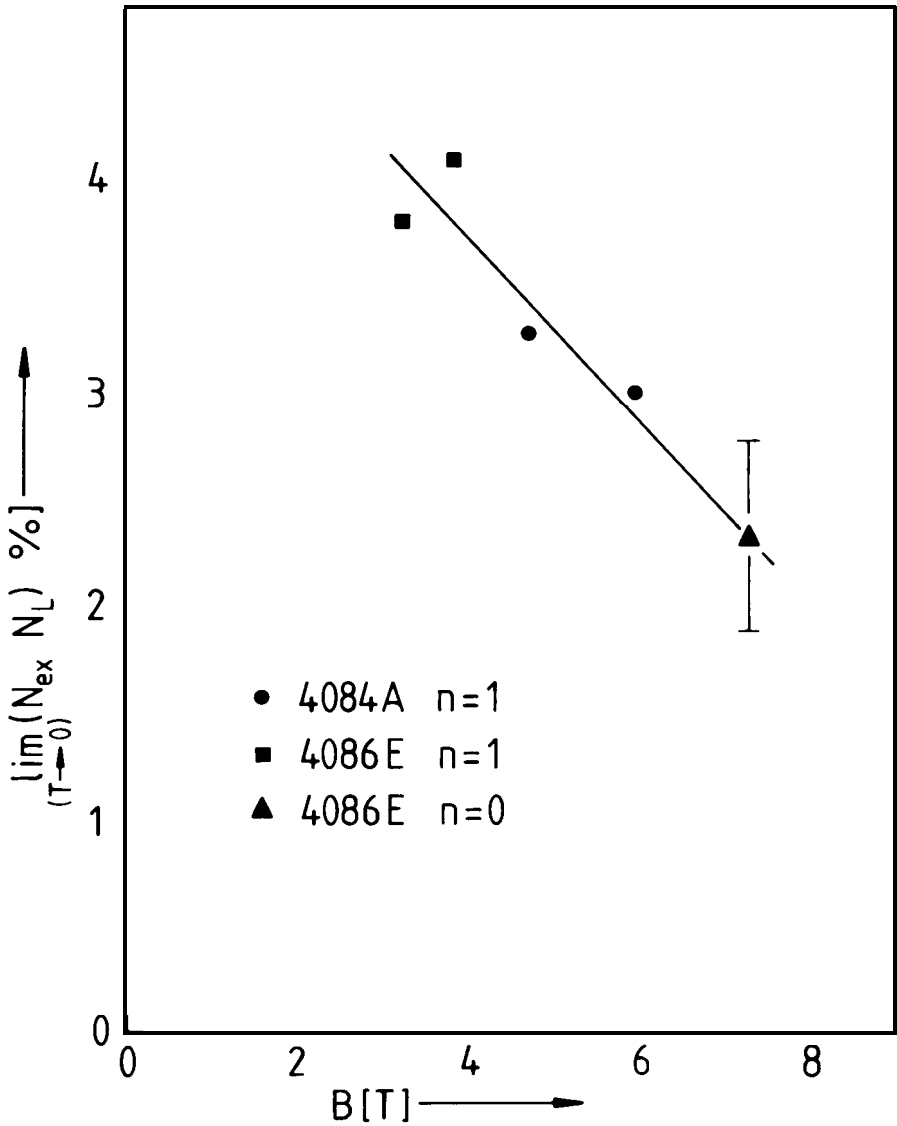


Fig. 15. Fraction of extended states relative to the number of states of one Landau level as a function of the magnetic field.

by the same activation energy as found for  $\rho_{xx}(T)$ . Experimentally [35], a one to one relation between the minimal resistivity  $\rho_{xx}^{\min}$  at integer filling factors and the slope of the Hall plateau has been found (Fig. 21) so that the flatness of the plateau increases with decreasing resistivity, which means lower temperature or higher magnetic fields.

The temperature dependence of the resistivity for Fermi energies within the mobility gap deviates from an activated behaviour at low temperatures, typically at  $T < 1\text{K}$ . Such deviations are found in measurements on disordered

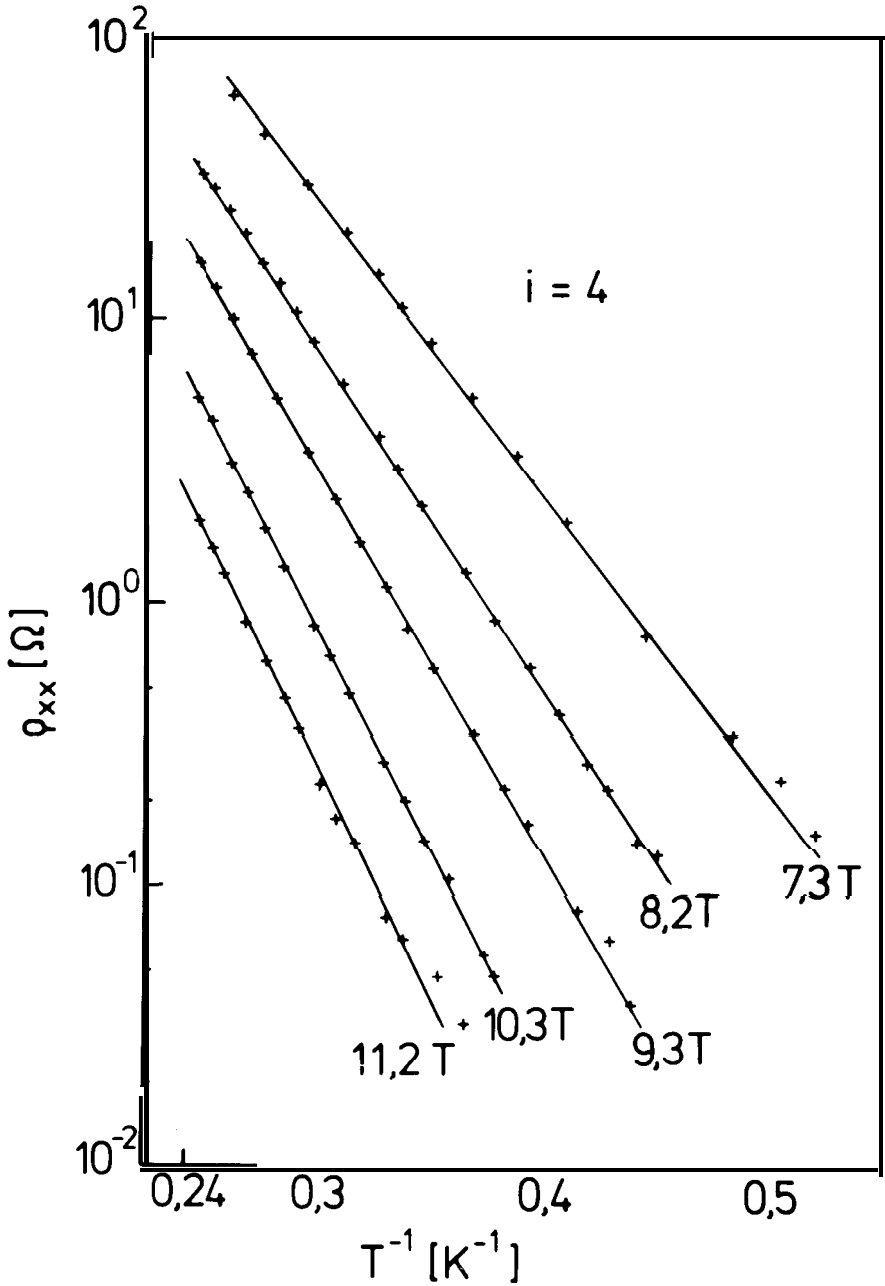


Fig 16. Thermally activated resistivity  $\rho_{xx}$  at a filling factor  $i = 4$  for a silicon MOSFET at different magnetic field values.

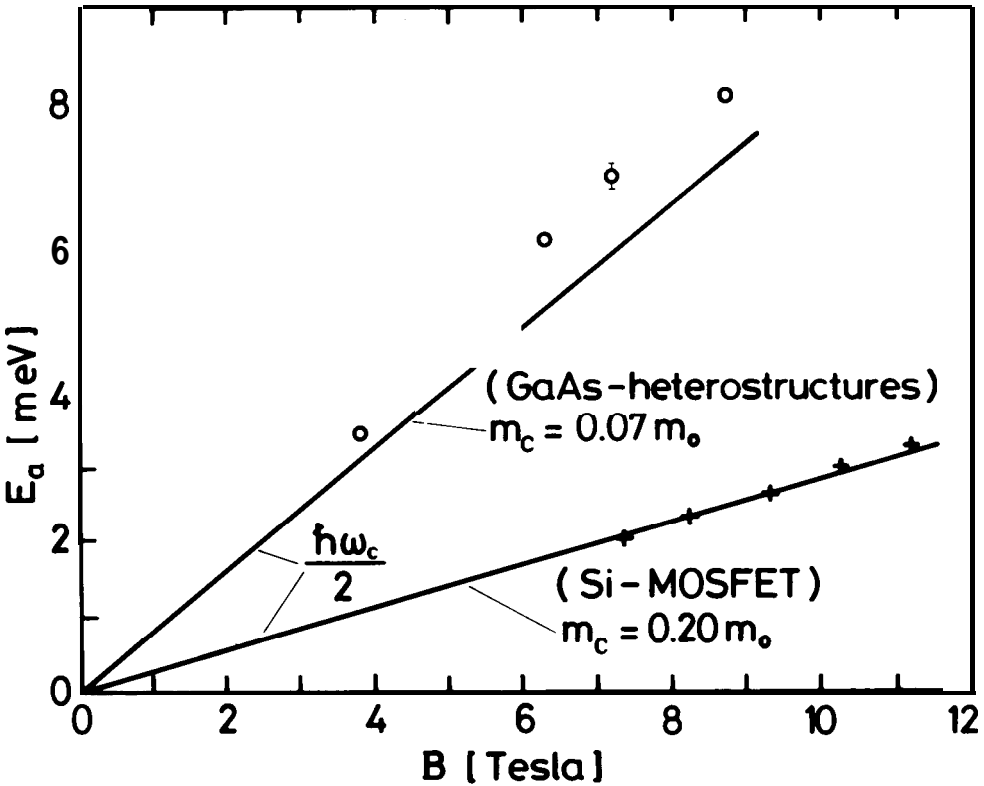


Fig. 17. Measured activation energies at filling factors  $i = 2$  (GaAs heterostructure) or  $i = 4$  (Si-MOSFET) as a function of the magnetic field. The data are compared with the energy  $0,5\hbar\omega_c$ .

systems, too, and are interpreted as variable range hopping. For a two-dimensional system with exponentially localized states a behaviour

$$\rho_{xx} \sim \exp [-(T_0/T)^{1/3}] \quad (20)$$

is expected. For a Gaussian localization the following dependence is predicted [36, 37]

$$\rho_{xx} \sim \frac{1}{T} \exp \{-(T_0/T)^{1/2}\} \quad (21)$$

The analysis of the experimental data demonstrates (Fig. 22) that the measurements are best described on the basis of Eq. (21). The same behaviour has been found in measurements on another two-dimensional system, on InP-InGaAs heterostructures [38].

The contribution of the variable range hopping (VRH) process to the Hall effect is negligibly small [39] so that experimentally the temperature dependence of  $dQ_{xy}/dn_s$  remains thermally activated even if the resistivity  $\rho_{xx}$  is dominated by VRH.

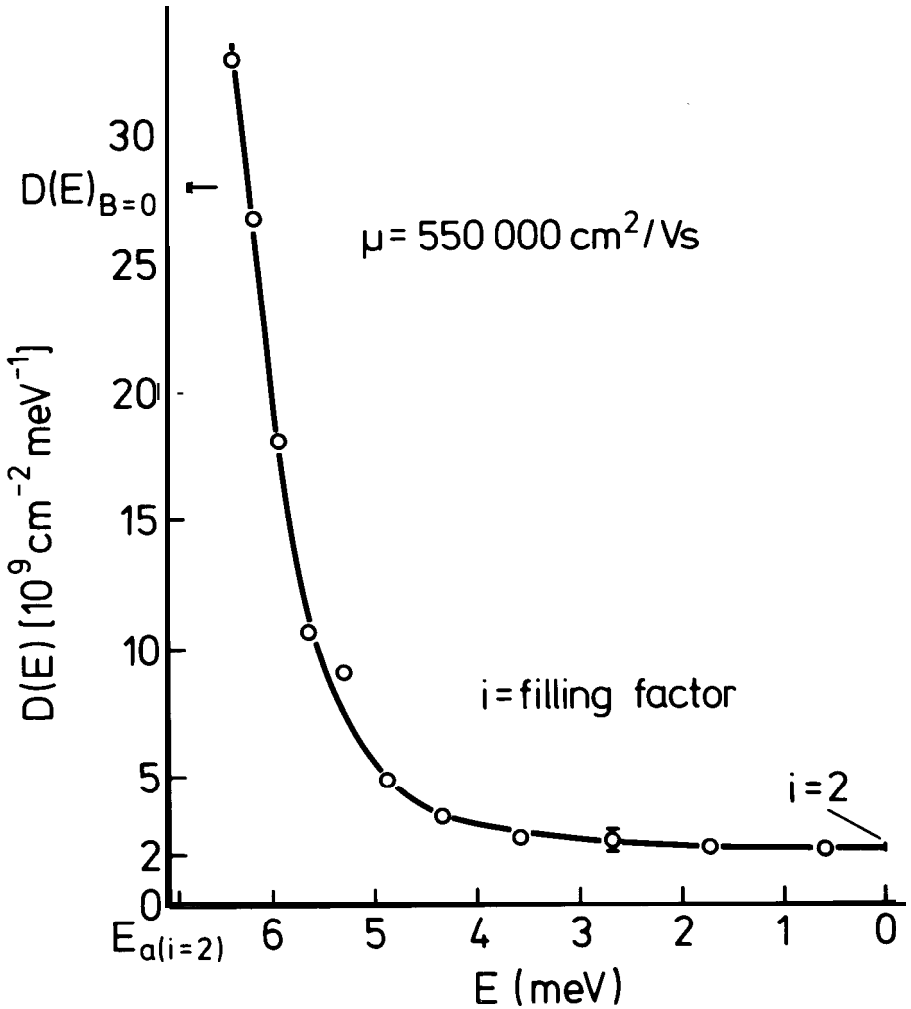


Fig. 18. Measured density of states (deduced from an analysis of the activated resistivity) as a function of the energy relative to the center between two Landau levels (GaAs-heterostructure).

The QHE breaks down if the Hall field becomes larger than about  $E_H = 60 \text{ V/cm}$  at magnetic fields of 5 Tesla.

This corresponds to a classical drift velocity  $v_D = \frac{E_H}{B} \approx 1200 \text{ m/s}$ . At the critical Hall field  $E_H$  (or current density  $j$ ) the resistivity increases abruptly by orders of magnitude and the Hall plateau disappears. This phenomenon has been observed by different authors for different materials [40-47]. A typical result is shown in Fig. 23. At a current density of  $j_c = 0.5 \text{ A/m}$  the resistivity  $\rho_{xx}$  at the center of the plateau (filling factor  $i = 2$ ) increases drastically. This instability, which develops within a time scale of less than 100 ns seems to originate from a runaway in the electron temperature but also other mechanism like electric field dependent delocalization, Zener tunneling or emission of

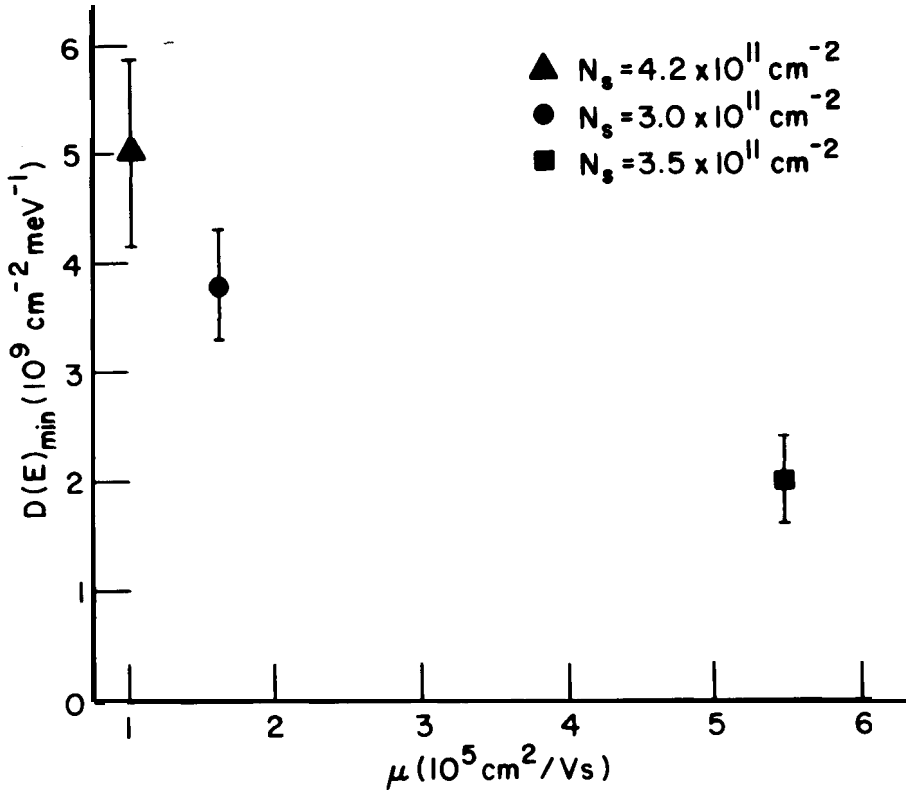


Fig. 19. Background density of states as a function of the mobility of the device.

acoustic phonons, if the drift velocity exceeds the sound velocity, can be used for an explanation [48-50].

Fig. 23 shows that  $\rho_{xx}$  increases already at current densities well below the critical value  $j_c$  which may be explained by a broadening of the extended state region and therefore a reduction in the mobility gap  $\Delta E$ . If the resistivity  $\rho_{xx}$  is thermally activated and the mobility gap changes linearly with the Hall field (which is proportional to the current density  $j$ ) then a variation

$$\ln \rho_{xx} \sim j$$

is expected. Such a dependence is seen in Fig. 24 but a quantitative analysis is difficult since the current distribution within the sample is usually inhomogeneous and the Hall field, calculated from the Hall voltage and the width of the sample, represents only a mean value. Even for an ideal two-dimensional system an inhomogeneous Hall potential distribution across the width of the sample is expected [51-53] with an enhancement of the current density close to the boundaries of the sample.

The experimental situation is still more complicated as shown in Fig. 25. The potential distribution depends strongly on the magnetic field. Within the plateau region the current path moves with increasing magnetic field across the

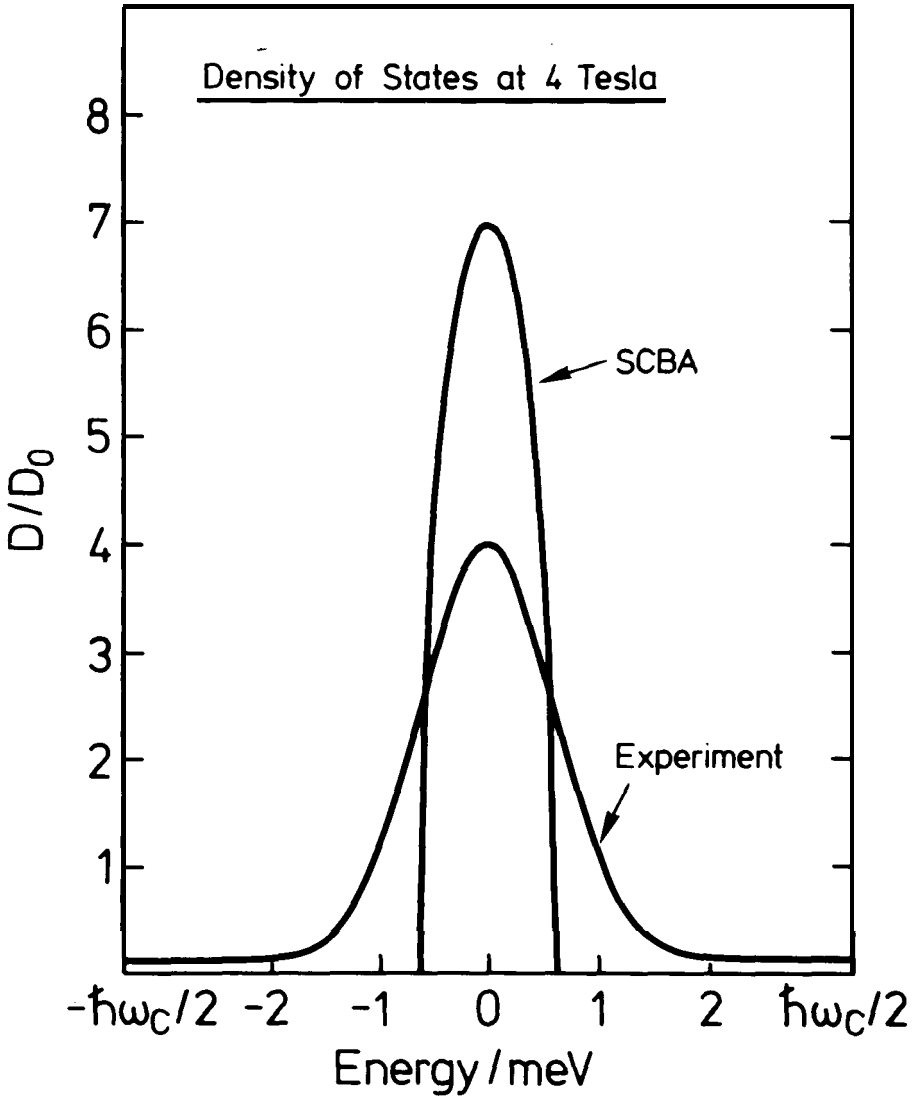


Fig. 20. Experimentally deduced density of states of a GaAs heterostructure at  $B = 4\text{T}$  compared with the calculated result based on the self-consistent Born approximation (SCBA).

width of the sample from one edge to the other one. A gradient in the carrier density within the two-dimensional system seems to be the most plausible explanation but in addition an inhomogeneity produced by the current itself may play a role. Up to now, not enough microscopic details about the two-dimensional system are known so that at present a microscopic theory, which describes the QHE under real experimental conditions, is not available. However, all experiments and theories indicate that in the limit of vanishing resistivity  $\rho_{xx}$  the value of the quantized Hall resistance depends exclusively on fundamental constants. This leads to a direct application of the QHE in metrology.

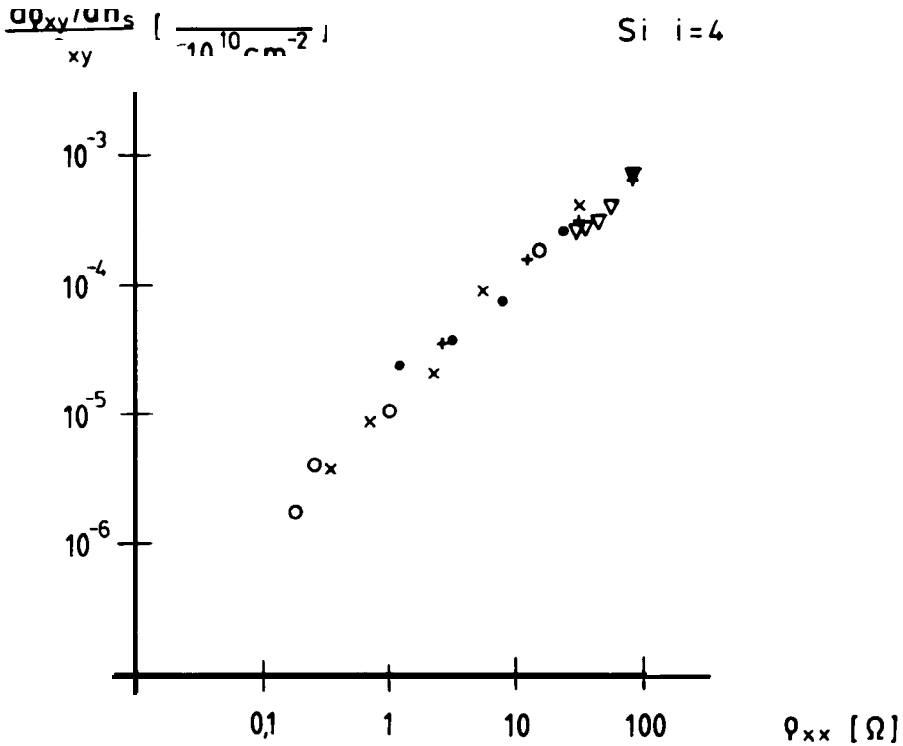


Fig. 21. Relation between the slope of the Hall plateaus  $d\rho_{xy}/dn_s$  and the corresponding  $\rho_{xx}$ -value at integer filling factors.

### 5. Application of the Quantum Hall Effect in Metrology

The applications of the Quantum Hall Effect are very similar to the applications of the Josephson-Effect which can be used for the determination of the fundamental constant  $h/e$  or for the realization of a voltage standard. In analogy, the QHE can be used for a determination of  $h/e^2$  or as a resistance standard. [54].

Since the inverse fine structure constant  $\alpha^{-1}$  is more or less identical with  $h/e^2$  (the proportional constant is a fixed number which includes the velocity of light), high precision measurements of the quantized Hall resistance are important for all areas in physics which are connected with the finestructure constant.

Experimentally, the precision measurement of  $a$  is reduced to the problem of measuring an electrical resistance with high accuracy and the different methods and results are summarized in the Proceedings of the 1984 Conference on Precision Electromagnetic Measurements (CPEM 84) [55]. The mean value of measurements at laboratories in three different countries is

$$\alpha^{-1} = 137,035988 \pm 0.00002$$

The internationally recommended value (1973) is

$$\alpha^{-1} = 137,03604 \pm 0.00011$$

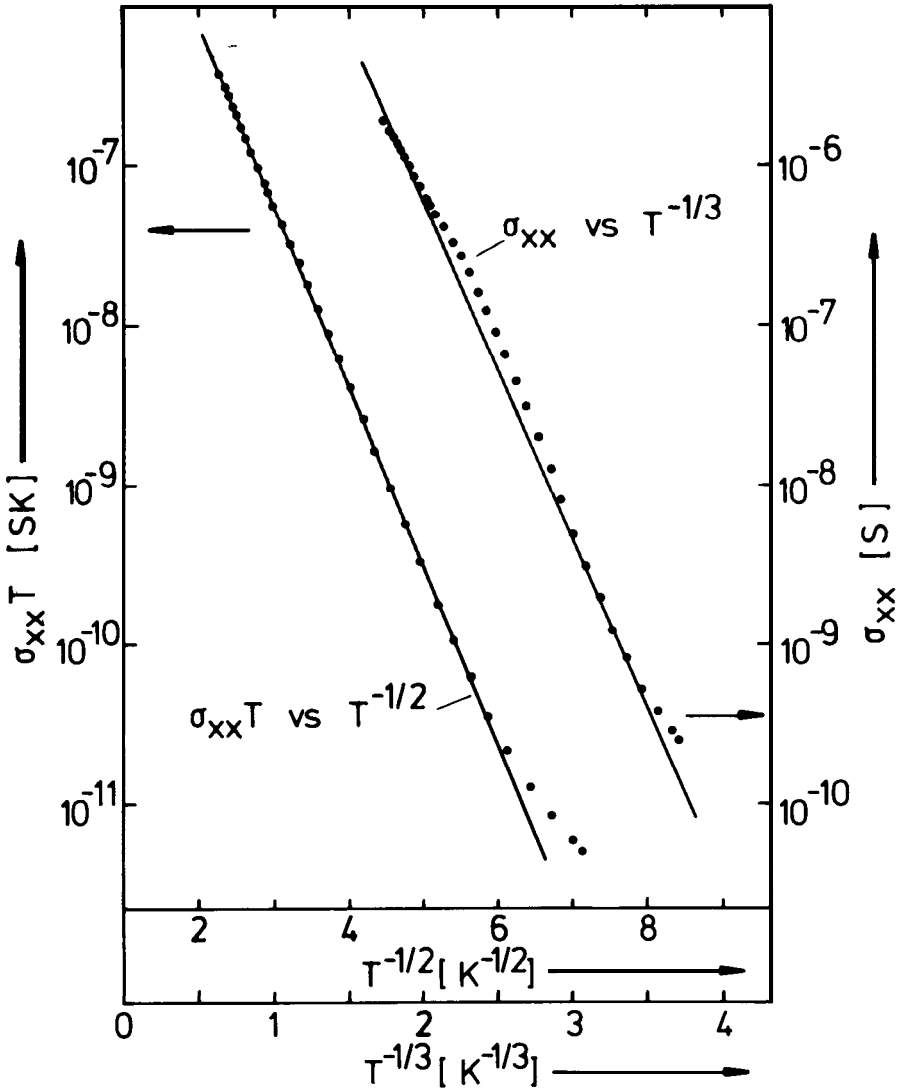


Fig. 22. Analysis of the temperature dependent conductivity of a GaAs heterostructure (filling factor  $i = 3$ ) at  $T < 0,2\text{K}$ .

and the preliminary value for the tinsturcture constant based on a new least square adjustment of fundamental constants (1985) is

$$\alpha^{-1} = 137,035991 \pm 0.000008$$

Different groups have demonstrated that the experimental result is within the experimental uncertainty of less than  $3.7 \cdot 10^3$  independent of the material (Si, GaAs,  $\text{In}_{0.53}\text{Ga}_{0.47}\text{As}$ ) and of the growing technique of the devices (MBE or MOCVD) [56]. The main problem in high precision measurements of  $\alpha$  is-at present-the calibration and stability of the reference resistor. Fig. 26 shows the drift of the maintained  $1\Omega$ -resistor at different national laboratories. The



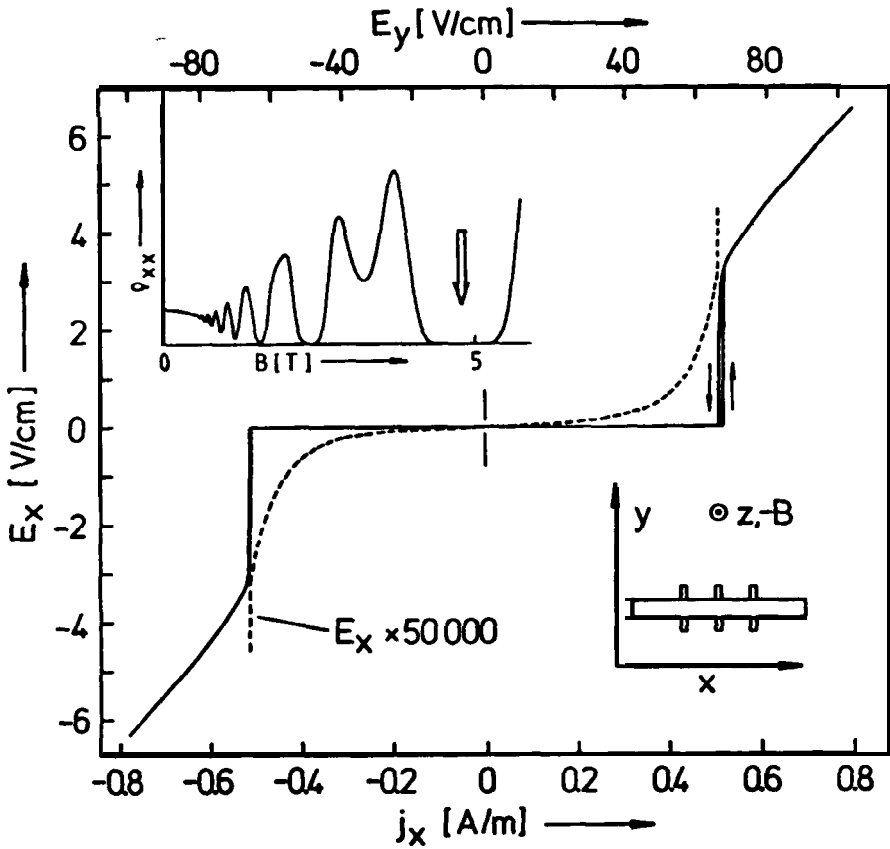


Fig. 23. Current-voltage characteristic of a GaAs-Al<sub>x</sub>Ga<sub>1-x</sub>As heterostructure at a filling factor  $\nu = 2$  ( $T = 1.4\text{K}$ ). The device geometry and the  $\rho_{xx}(B)$ -curve are shown in the inserts.

very first application of the QHE is the determination of the drift coefficient of the standard resistors since the quantized Hall resistance is more stable and more reproducible than any wire resistor. A nice demonstration of such an application is shown in Fig. 27. In this experiment the quantized Hall resistance  $R_H$  has been measured at the "Physikalisch Technische Bundesanstalt" relative to a reference resistor  $R_R$  as a function of time. The ratio  $R_H/R_R$  changes approximately linearly with time but the result is independent of the QHE-sample. This demonstrates that the reference resistor changes its value with time. The one standard deviation of the experimental data from the mean value is only  $2.4 \cdot 10^{-8}$  so that the QHE can be used already today as a relative standard to maintain a laboratory unit of resistance based on wire-wound resistors. There exists an agreement that the QHE should be used as an absolute resistance standard if three independent laboratories measure the same value for the quantized Hall resistance (in SI-units) with an uncertainty of less than  $2 \cdot 10^{-7}$ . It is expected that these measurements will be finished until the end of 1986.

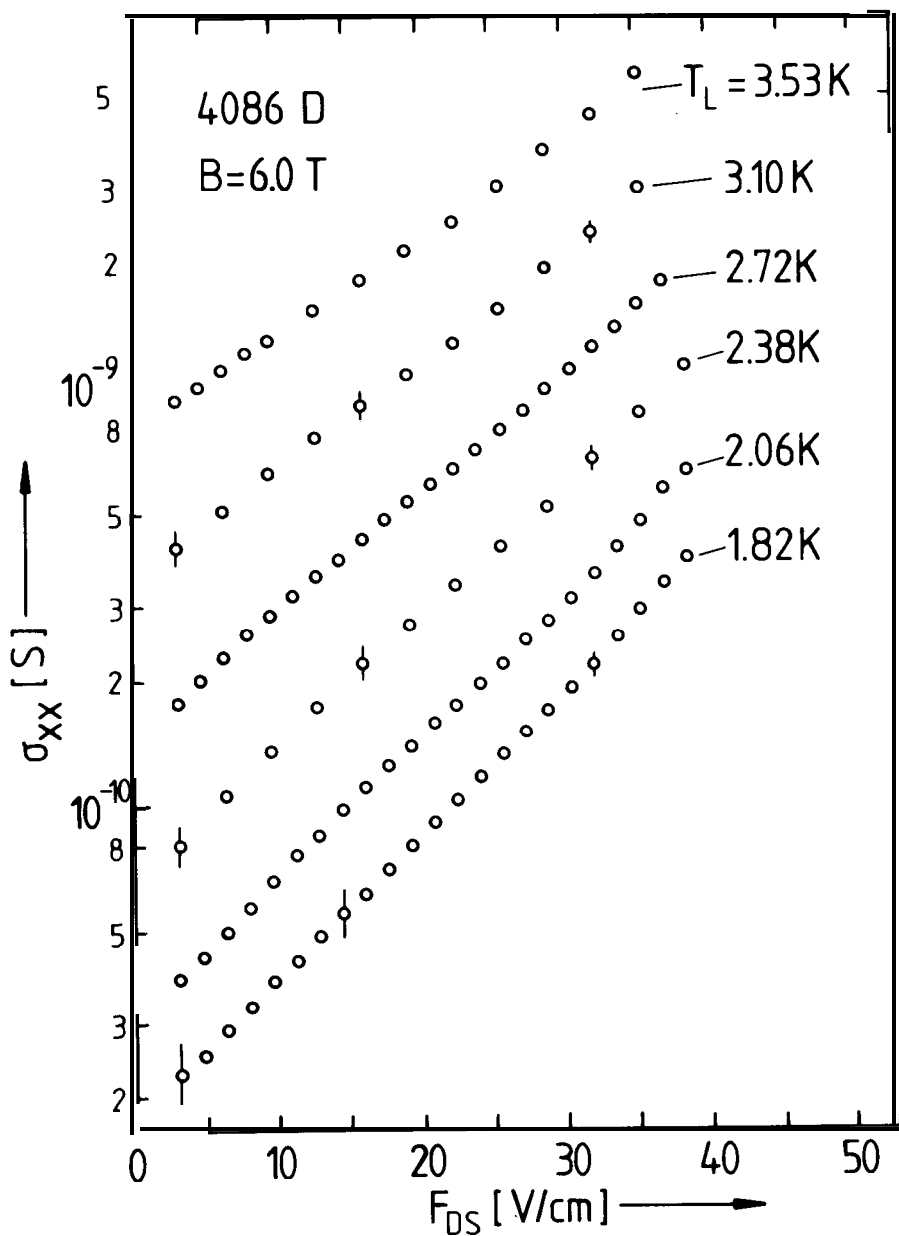


Fig. 24. Nonohmic conductivity  $\sigma_{xx}$  of a GaAs heterostructure at different temperatures  $T_L$  (filling factor  $\nu = 2$ ). An instability is observed at source-drain fields larger than 40 V/cm.

#### Acknowledgements

The publicity of the Nobel Prize has made clear that the research work connected with the Quantum Hall Effect was so successful because a tremendous large number of institutions and individuals supported this activity. I would like to thank all of them and I will mention by name only those scientists who supported my research work at the time of the discovery of the QHE in

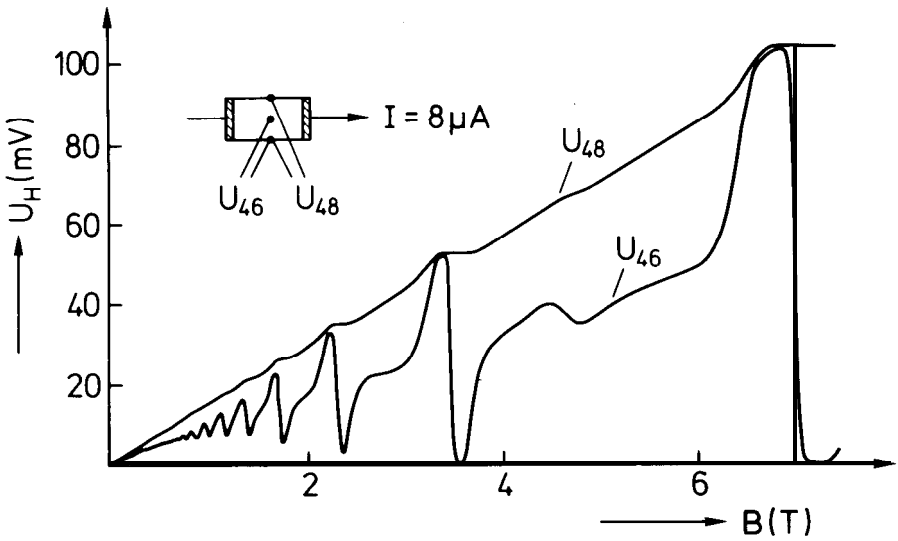


Fig. 25. Measured Hall potential distribution of a GaAs heterostructure as a function of the magnetic field.

1980. Primarily, I would like to thank G. Dorda (Siemens Forschungslaboratorien) and M. Pepper (Cavendish Laboratory, Cambridge) for providing me with high quality MOS-devices. The continuous support of my research work by G. Landwehr and the fruitful discussions with my coworker, Th. Englert, were essential for the discovery of the Quantum Hall Effect and are gratefully acknowledged.

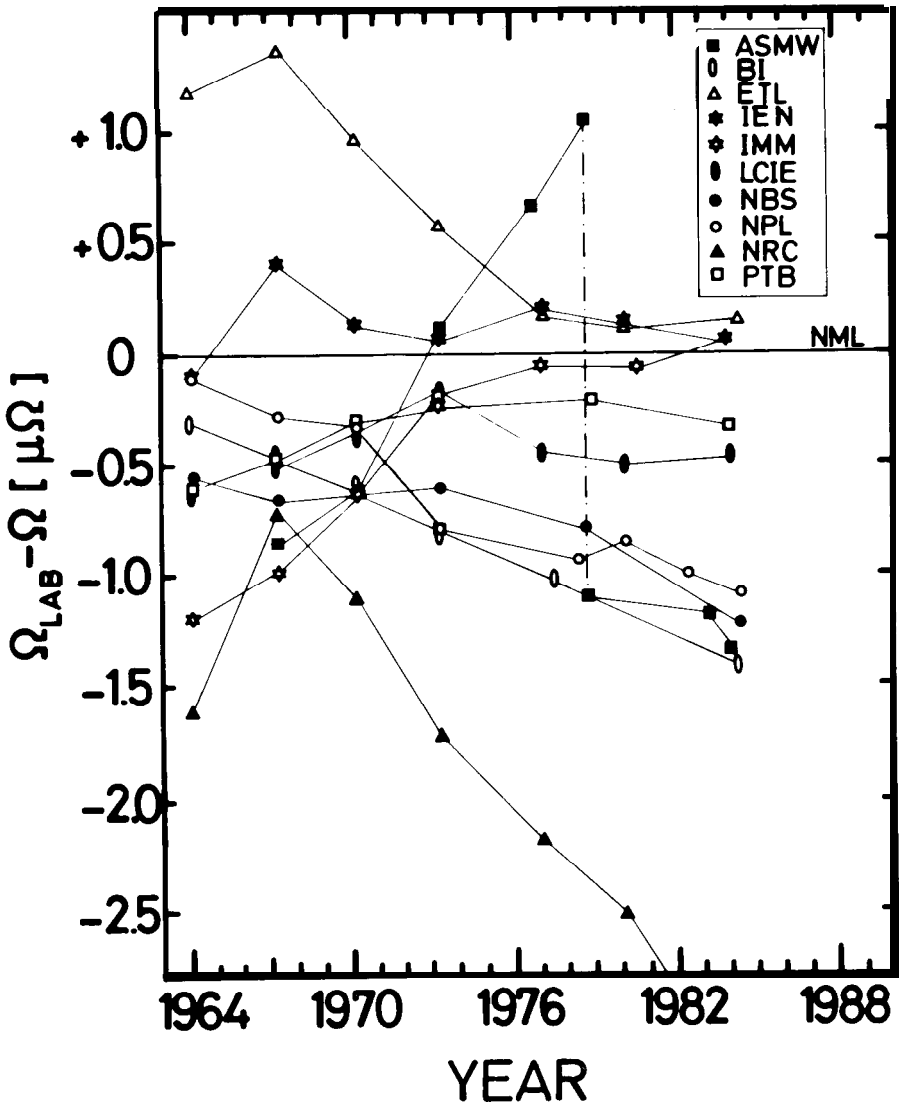


Fig. 26. Time dependence of the  $I\Omega$  standard resistors maintained at the different national laboratories.

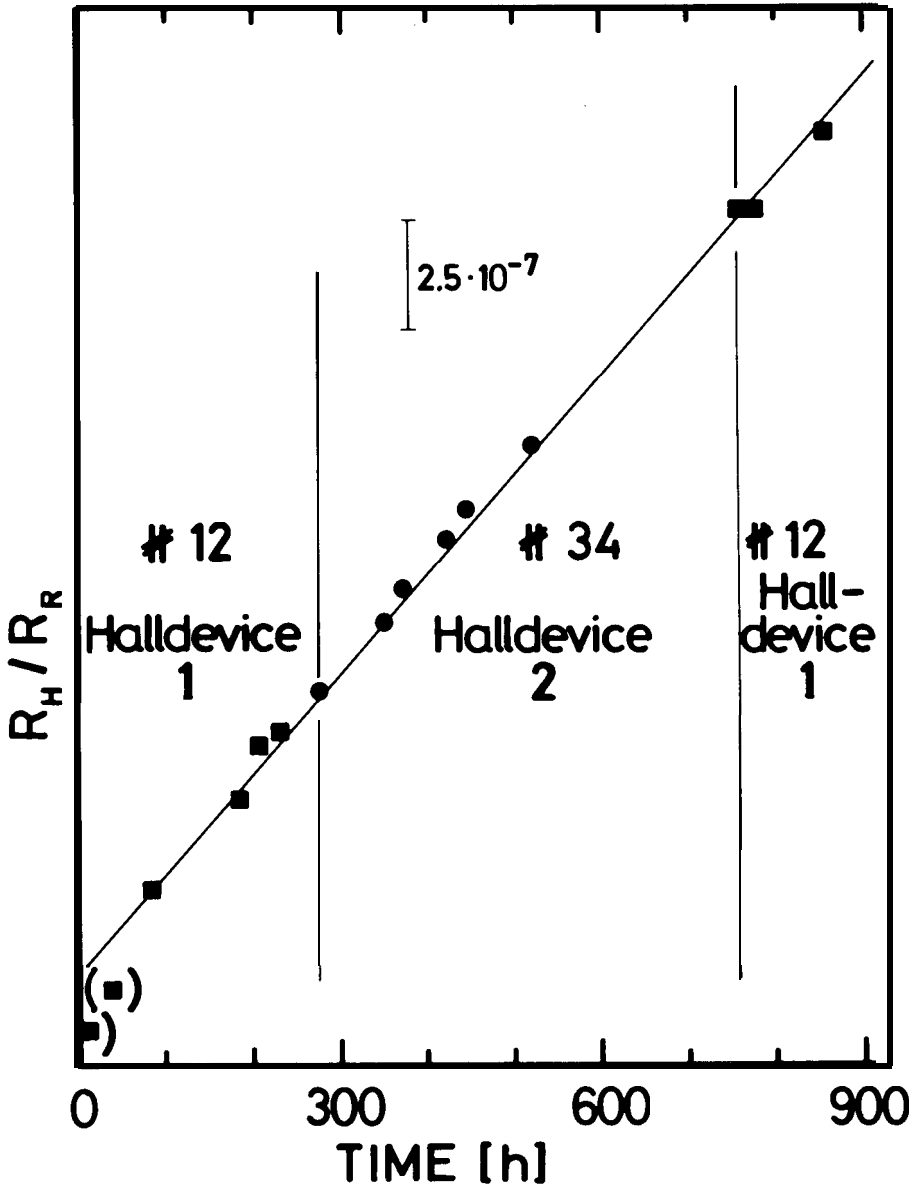


Fig. 27. Ratio  $R_H/R_R$  between the quantized Hall resistance  $R_H$  and a wire resistor  $R_R$  as a function of time. The result is time dependent but independent of the Hall device used in the experiment.

## REFERENCES

- [ 1 ] A.B. Fowler, F.F. Fang, W.E. Howard and P.J. Stiles Phys. Rev. Letter 16, 901 ( 1966)
- [ 21 ] For a review see: Proceedings of the Int. Conf. on Electronic Properties of Two-Dimensional Systems, Surf. Sci. 58, (1976), 73 (1978), 98 (1980), 113 (1982), **142 (1984)**
- [ 31 ] F. Stern and W.E. Howard, Phys. Rev. 163, 816 (1967)
- [ 41 ] T. Ando, J. Phys. Soc., Jpn. 51, 3893 (1982)
- [ 51 ] J.F. Koch, Festkörperprobleme (Advances in Solid State Physics), H.J. Queisser, Ed. (Pergamon-Vieweg, Braunschweig, 1975) Vol. XV, p. 79
- [ 61 ] T. Mimura, Surf. Science **113**, **454** (1982)
- [ 71 ] R.B. Laughlin, Surface Science **113**, **22** (1982)
- [ 81 ] R. Kubo, S.J. Miyake and N. Hashitsume, in Solid State Physics, Vol. 17, 269 (1965). F. Seitz and D. Turnbull, Eds., (Academic Press, New York, 1965)
- [ 91 ] T. Ando, J. Phys. Soc. Jpn. 37, 1233 (1974)
- [10] R. B. Laughlin in Springer Series in Solid State Sciences 53, p. 272, G. Bauer, F. Kuchar and H. Heinrich, Eds. (Springer Verlag, 1984)
- [11] R.E. Prange, Phys. Rev. B 23, 4802 (1981)
- [12] H. Aoki and T. Ando, Solid State Commun. 38, 1079 (1981)
- [13] J. T. Chalker, J. Phys. C 16, 4297 (1983)
- [14] W. Brenig, Z. Phys. .50B, 305 (1983)
- [15] A. Mac Kinnon, L. Schweitzer and B. Kramer, Surf. Sci. **142**, 189 (1984)
- [16] T. Ando, J. Phys. Soc. Jpn. 52, 1740 (1983)
- [17] L. Schweitzer, B. Kramer and A. Mac Kinnon, J. Phys. C 17, 4111 (1984)
- [18] H. Aoki and T. Ando, Phys. Rev. Letters 54, 831 (1985)
- [19] E. Abrahams, P.W. Anderson, D.C. Licciardello and T.V. Ramakrishnan, Phys. Rev. Letters 42, 673 (1979)
- [20] G.A. Baraff and D.C. Tsui, Phys. Rev. B 24, 2274 (1981)
- [21] T. Toyoda, V. Gudmundsson and Y. Takahashi, Phys. Letters **102A**, 130 (1984)
- [22] S. Kawaji and J. Wakabayashi, Surf. Sci. 58, 238 (1976)
- [23] S. Kawaji, T. Igarashi and J. Wakabayashi, Progr. in Theoretical Physics 57, 176 (1975)
- [24] T. Englert and K. v. Klitzing, Surf. Sci. 73, 70 (1978)
- [25] K. v. Klitzing, G. Dorda and M. Pepper, Phys. Rev. Letters 45, 494 (1980)
- [26] K. v. Klitzing, H. Obloh, G. Ebert, J. Knecht and K. Ploog, Prec. Measurement and Fundamental Constants II, B.N. Taylor and W.D. Phillips, Eds., Natl. Bur. Stand. (U.S.), Spec. Publ. **617**, (1984) p. 526
- [27] R.W. Rendell and S.M. Girvin, Prec. Measurement and Fundamental Constants II, B.N. Taylor and W.D. Phillips, Eds. Natl. Bur. Stand. (U.S.), Spec. Publ. **617**, (1984) p. 557
- [28] K. v. Klitzing, Festkörperprobleme (Advances in Solid State Physics), XXI, 1 (1981), J. Treusch, Ed., (Vieweg, Braunschweig)
- [29] G. Ebert, K. v. Klitzing, C. Probst and K. Ploog, Solid State Commun. 44, 95 (1982)
- [30] E. Stahl, D. Weiss, G. Weimann, K. v. Klitzing and K. Ploog, J. Phys. C **18**, L 783 (1985)
- [31] T.P. Smith, B.B. Goldberg, P.J. Stiles and M. Heiblum, Phys. Rev. B 32, 2696 (1985)
- [32] V. Mosser, D. Weiss, K. v. Klitzing, K. Ploog and G. Weimann to be published in Solid State Commun.
- [33] E. Gornik, R. Lassnig, G. Strasser, H.L. Störmer, A.C. Gossard and W. Wiegmann, Phys. Rev. Lett. 54, 1820 (1985)
- [34] J.P. Eisenstein, H.L. Störmer, V. Navayanamurti, A.Y. Cho and A.C. Gossard, Yamada Conf. XIII on Electronic Properties of Two-Dimensional Systems, p. 292 (1985)

- [35] B. Tausendfreund and K. v. Klitzing, Surf. Science 142, 220 (1984)
- [36] M. Pepper, Philos. Mag. 37, 83 (1978)
- [37] Y. Ono, J. Phys. Soc. Jpn. 51, 237 (1982)
- [38] Y. Guldner, J.P. Hirtz, A. Briggs, J.P. Vieren, M. Voos and M. Razeghi, Surf. Science **142, 179 (1984)**
- [39] K.I. Wysokinski and W. Brenig, Z. Phys. B - Condensed Matter 54, 11 (1983)
- [40] G. Ebert and K. v. Klitzing, J. Phys. C 5441 (1983)
- [41] M.E. Cage, R.F. Dziuba, B.F. Field, E.R. Williams, S.M. Girvin, A.C. Gossard, D.C. Tsui and R.J. Wagner, Phys. Rev. Letters 51, 1374 (1983)
- [42] F. Kuchar, G. Bauer, G. Weimann and H. Burkhard, Surf. Science 142, 196 (1984)
- [43] H.L. Störmer, A.M. Chang, D.C. Tsui and J.C.M. Hwang, Proc. 17th ICPS, San Francisco 1984
- [44] H. Sakaki, K. Hirakawa, J. Yoshino, S.P. Svensson, Y. Sekiguchi, T. Hotta and S. Nishii, Surf. Science **142, 306 (1984)**
- [45] K v. Klitzing, G. Ebert, N. Kleinmichel, H. Obloh, G. Dorda and G. Weimann, Proc. 17th ICPS, San Francisco 1984
- [46] F. Kuchar, R. Meisels, G. Weimann and H. Burkhard, Proc. 17th ICPS, San Francisco 1984
- [47] V.M. Pudalov and S.G. Semenchinsky, Solid State Commun. 51, 19 (1984)
- [48] P. Streda and K. v. Klitzing, J. Phys. C 17, L 483 (1984)
- [49] O. Heinonen, P.L. Taylor and S.M. Girvin, Phys. Rev. B 30, 3016 (1984)
- [50] S.A. Trugman, Phys. Rev. B 27, 7539 (1983)
- [51] A.H. Mac Donald, T.M. Rice and W.F. Brinkman, Phys. Rev. B 28, 3648 (1983)
- [52] O. Heinonen and P.L. Taylor, Phys. Rev. B 32, 633 (1985)
- [53] J. Riess, J. Phys. C **17**, L 849 (1984)
- [54] K. v. Klitzing and G. Ebert, Metrologia 21, 11 (1985)
- [55] High-precision measurements of the quantized Hall resistance are summarized in: IEEE Trans. Instrum. Meas. IM 34, pp. 301-327
- [56] F. Delahaye, D. Dominguez, F. Alexandre, J. P. Andre, J. P. Hirtz and M. Razeghi, Metrologia 22, 103 (1986)